Valence variations in titanium-based perovskite oxides by high-pressure and high-temperature method

doi: 10.1557/JMR.2001.0063

Valence variations in titanium-based perovskite oxides by high-pressure and high-temperature method

Liping Li
Department of Physics, Jilin University, Changchun 130023, People's Republic of China

Guangshe Li[a)]
Research Center of Supercritical Fluid Technology, Department of Chemical Engineering, Tohoku University, Sendai 980-8579, Japan

Jipeng Miao and Wenhui Su
Department of Physics, Jilin University, Changchun 130023, People's Republic of China

Hiroshi Inomata
Research Center of Supercritical Fluid Technology, Department of Chemical Engineering, Tohoku University, Sendai 980-8579, Japan

(Received 1 November 1999; accepted 30 October 2000)

Typical titanium-based perovskite oxides $Eu_{1-x}Ba_xTiO_3$ ($x = 0.6$–0.8), $Eu_{1-x}K_xTiO_3$ ($x = 0.2$,0.32), and $La_{0.7}(Na,K)_{0.3}TiO_3$ were synthesized by high pressure and temperature using RE_2O_3 (RE = La,Eu), TiO_2, alkaline, or alkaline earth carbonates as the starting materials. X-ray diffraction data analysis showed that there was a structural transformation in $Eu_{1-x}Ba_xTiO_3$ by varying Ba content [i.e., from cubic ($x = 0.6$,0.7) to tetragonal ($x = 0.8$)], and that samples $Eu_{1-x}K_xTiO_3$ and $La_{0.7}(Na,K)_{0.3}TiO_3$ crystallized in the cubic perovskite structure. ^{151}Eu Mössbauer spectroscopy and electron paramagnetic resonance measurements revealed mixed valence of Eu^{2+}/Eu^{3+} in samples $Eu_{1-x}Ba_xTiO_3$ and $Eu_{1-x}K_xTiO_3$, while Ti ions were present in pure Ti^{4+} state. Cubic $Eu_{1-x}K_xTiO_3$ was metastable, which decomposed into a mixture of perovskite and pyrochlore phases at high temperatures as accompanied by an oxidation process from Eu^{2+} to Eu^{3+}. For samples $La_{0.7}(Na,K)_{0.3}TiO_3$, Ti^{3+} signals were clearly observed. The reduction mechanisms for Eu ions at A site and Ti ions at B site in the perovskite oxides are discussed in terms of the chemical nature of the framework ions and substitution ions under high pressure and temperature.

I. INTRODUCTION

Mixed valence characteristics of the rare-earth and transition-metal ions in ceramic materials have been paid more attention to due to the correlating excellent physical properties. The valence states for rare-earth and transition elements characterize the average number of *f* or *d* electron bonding with the neighboring anionic groups. In fact, the valence natures are strongly influenced by the structural factors (e.g., the ionic size and lattice symmetry), the properties of chemical bonding, and the electron configurations of the dopants. It is well accepted that the framework ions in the oxide materials could be stabilized in certain valence states by varying the experimental conditions and chemical compositions. A strong correlation can be therefore expected among electronic interactions, crystal structures, and external temperatures and pressures. Some interesting physical phenomena including pressure-induced structural transformations, pressure-induced electronic transitions, and so on have come to light in the compounds containing rare-earth elements (e.g., Eu).[1]

For the perovskite structure ABO_3, BO_6 octahedron build up the stable skeleton, while A-site ions occupy the interstices of the skeleton. These framework ions being stabilized in specific valences account for the controllable structures and physical properties. High pressure is considered as an effective method for the stabilization of certain valence states. For example, by high oxygen pressures,[2–4] the perovskite oxides containing transition-metal ions (e.g., Cu, Fe, Cr) with the unusual valence states have been obtained. Alternatively, some reduction reactions can also occur by stabilizing certain lower valence ions under high pressure and temperature.[5] Recently, we stabilized pure trivalent dopants in ceria lattice at a pressure of 3.6 GPa and in a temperature range of 900–1000 °C.[6] We believe that high pressure and tem-

[a)]Address all correspondence to this author.
e-mail: guangshe@scf.che.tohoku.ac.jp

perature might play some significant roles in creating mixed valences of rare-earth and transition ions during the synthetic procedure of the perovskite oxides. However, there are few systematic studies on the effects of the dopants on the lower valence ions as stabilized by high pressure and temperature.

In this article, we report on the valence variations of Eu ions at A site and Ti ions at B site in several typical titanium-based perovskite oxides [e.g., $Eu_{1-x}Ba_xTiO_3$ ($x = 0.6$–0.8), $Eu_{1-x}K_xTiO_3$, and $La_{0.7}(Na,K)_{0.3}TiO_3$] with an aim to further determine the mixed valence characteristics of Eu and Ti ions and the structural stabilities of the Ti-based perovskite oxides obtained by high pressure and temperature.

II. EXPERIMENTAL PROCEDURE

Chemicals Eu_2O_3, La_2O_3, TiO_2, $BaCO_3$, and $MHCO_3$ (M = Na,K) were used as the starting materials. They were weighed according to the nominal ratios of $Eu_{1-x}Ba_xTiO_3$ ($x = 0.6$–0.8), $Eu_{1-x}K_xTiO_3$ ($x = 0.2,0.32$), and $La_{0.7}(Na,K)_{0.3}TiO_3$. After thoroughly mixing, the mixtures were heated to 900 °C for 5 h at ambient pressure so as to decompose completely the carbonates and to initiate partial reactions. The decomposition products were detected by powder x-ray diffraction (XRD) to be the mixtures of perovskite phases and the component oxides. These mixtures were put into a high-pressure chamber as shown in Ref. 7. A belt-type apparatus was used to synthesize the samples. The pressure was loaded to 4.0 GPa. The temperature was then increased gradually to 900 °C. After being kept at high pressure and temperature for 15 min, the specimens were quenched to room temperature under high pressure. Finally the pressure was released.

Powder XRD data were collected at room temperature on a Rigaku 12-kW copper rotating x-ray diffractometer. The scanning rate was $0.02° \text{ min}^{-1}$. The lattice parameters were determined by least-squares methods.

^{151}Eu Mössbauer spectra of the samples were recorded at room temperature by means of an Oxford MS-500 constant acceleration spectrometer. The velocity was calibrated with an α–Fe foil. The radiation source was $^{151}Eu/SmF_3$. The thickness of the absorber used in the measurements was around 6–15 Eu mg/cm^2. The experimental Mössbauer data were fitted using superimposing Lorentzians.

Electron paramagnetic-resonance (EPR) spectra were recorded on a Bruker ER200D EPR spectrometer at room temperature. A frequency of approximately 9.77 GHz was used for a dual-purpose cavity operation. The magnetic field of 0.32 mT was modulated at 100 kHz. A microwave power of approximately 6.5 mW was employed. Reference signals of Mn^{2+} ions in MgO crystals were used as the standard for the precise effective gyromeznetic (g) factor value. The factor was defined experimentally as $h\nu/\beta H$, where ν is the microwave frequency, H is the magnetic field, h is the Plank constant, and β is the Bohr magneton.

The structural stabilities of the samples were studied by thermal gravimetric (TG) analysis on a TG-7 thermogravimetric analyzer at a heating rate of 10 °C min^{-1}.

III. RESULTS AND DISCUSSION

A. Structures and valence characteristics of the Ti-based perovskite samples by high pressure and temperature

Titanium-based perovskite oxides have showed significant structural transitions and physical properties.[8–10] Most of the polycrystalline samples containing dopants with quite different ionic size and valence states were prepared by arc-melting method using $Ti_2^{3+}O_3$ or metallic Ti^0 as the starting materials. Using this method, Ar or other inert gases are required for stabilizing the lower valence ions and for producing single phases. $Eu^{2+}Ti^{4+}O_3$ is a typical titanium-based oxide crystallizing in an ideal cubic perovskite lattice.[11] However, we found that it is very difficult to introduce some ions with much larger ionic size than Eu^{3+} at A site in $EuTiO_3$ lattice while keeping the single phase of perovskite structure when using the traditional high-temperature sintering method. This may be due to the changeable valence characteristics of Eu and Ti ions and the relatively high structural stabilities of the corresponding perovskite and pyrochlore phases. In the view of the fact that high pressure and temperature have some advantages in producing single-phase samples within a very short reaction time and furthermore in stabilizing lower valence states without any protection from inert gases, we prepared some typical Ti-based perovskite oxides by high pressure and temperature and studied the mixed valences of Eu^{2+}/Eu^{3+} at A site and Ti^{3+}/Ti^{4+} at B site.

XRD patterns for samples $Eu_{1-x}Ba_xTiO_3$, $Eu_{1-x}K_xTiO_3$, and $La_{0.7}M_{0.3}TiO_3$ (M = K,Na) by high pressure and temperature are shown in Fig. 1. Most of the intense diffraction peaks were highly symmetric. Analysis of the XRD data in Fig. 1(a) showed that samples $Eu_{1-x}Ba_xTiO_3$ ($x = 0.6$–0.8) and $Eu_{1-x}K_xTiO_3$ ($x = 0.2,0.32$) were single phases. For samples $La_{0.7}(Na,K)_{0.3}TiO_3$ as shown in Fig. 1(b) traces of component oxides TiO_2 or La_2O_3 were observed. Indexing results confirmed that $Eu_{1-x}Ba_xTiO_3$ ($x = 0.6,0.7$), $Eu_{1-x}K_xTiO_3$ ($x = 0.2,0.32$), and the main phase product of $La_{0.7}(Na,K)_{0.3}TiO_3$ crystallized in the cubic perovskite structures, whereas $Eu_{0.2}Ba_{0.8}TiO_3$ was determined to be in a tetragonal phase, which was manifested by the distinct splitting of the peak at a 2θ of approximately 45°.

The lattice parameters for the samples are listed in Table I. It is interesting that the lattice parameters for the samples seemed to be unaffected by Ba content. For examples, the lattice parameters for $Eu_{1-x}Ba_xTiO_3$ ($x = 0.6,0.7$) were near the same within the experimental error (i.e., $a = 0.396$ nm), which was slightly larger than that ($a = 0.391$ nm) for the parent $EuTiO_3$.[11] The latter case could be explained in terms of the larger ionic size of Ba^{2+} than that of Eu^{3+} or Eu^{2+}; alternatively the former case was closely related to the mixed valence of Eu^{2+}/Eu^{3+} in the lattice, as confirmed by the following EPR measurements. Substitution of Eu by Ba at A site could lead to an expansion of the perovskite lattice of $Eu_{1-x}Ba_xTiO_3$; however, Ti ions remained at B site as pure Ti^{4+}, therefore the appearance of Eu^{3+} ions in lattice probably resulted in a net positive charge on the octahedral layers by producing (i) cation vacancies at A site, which accounted for the lattice constraint, and (ii) interstitial oxygen species, which slightly increased the lattice volume and lattice distortion. As a consequence, the lattice parameters for samples $Eu_{1-x}Ba_xTiO_3$ remained near the same. Similar results have been found in samples $Eu_{1-x}K_xTiO_3$ ($x = 0.2,0.32$). But for $La_{0.7}(Na,K)_{0.3}TiO_3$, the similar lattice parameter was probably associated with the mixed valence of Ti^{3+}/Ti^{4+} at B site, which was confirmed by the following EPR measurements.

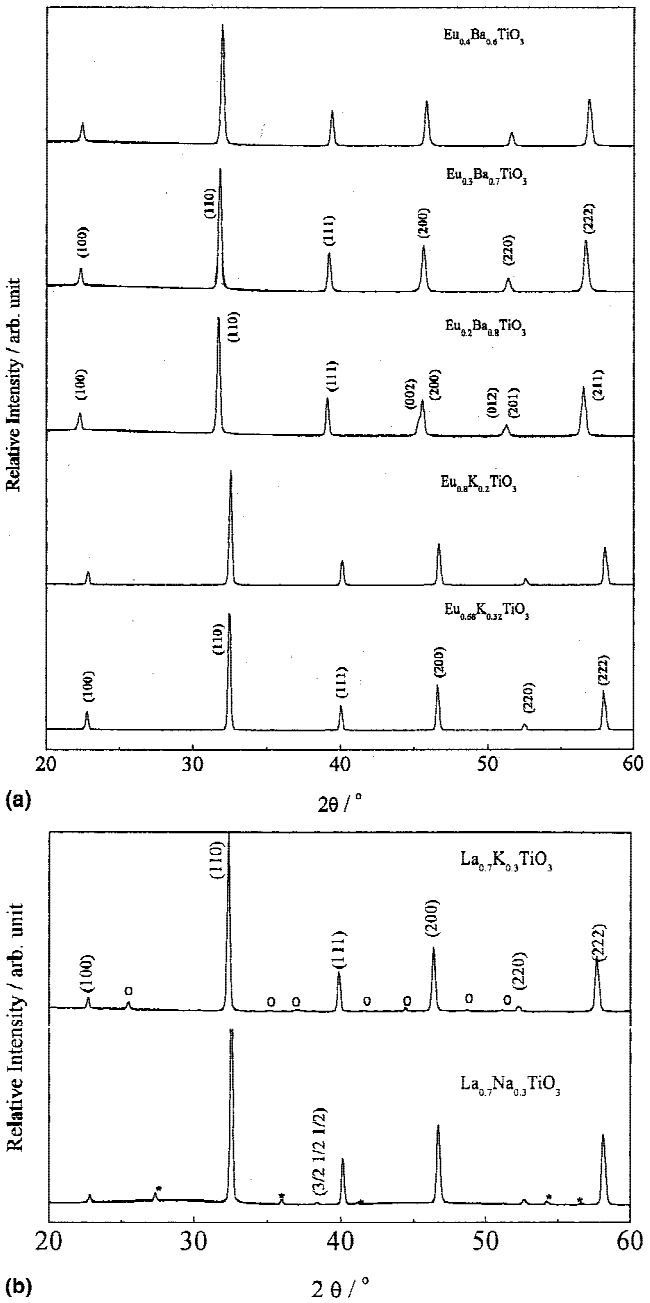

FIG. 1. XRD patterns for (a) $Eu_{1-x}Ba_xTiO_3$ ($x = 0.6$–0.8), $Eu_{1-x}K_xTiO_3$ ($x = 0.2,0.32$) and (b) $La_{0.7}(Na,K)_{0.3}TiO_3$ synthesized by high pressure and temperature. Circles and asterisks denote the diffraction peaks for components La_2O_3 and TiO_2, respectively.

For cubic $Eu_{1-x}Ba_xTiO_3$ ($x = 0.6,0.7$), $Eu_{1-x}K_xTiO_3$ ($x = 0.2,0.32$), and $La_{0.7}K_{0.3}TiO_3$, no superstructure diffraction peaks were observed by scaling up the XRD patterns in Fig. 1. This gave an indication that there were no obvious tilting TiO_6 octahedra in the lattice. For $La_{0.7}Na_{0.3}TiO_3$, however a very weak superstructure peak (3/2, 1/2, 1/2) at a 2θ of approximately 38° was observed, which was due to the tilting TiO_6 octahedra arrangements in perovskite lattice. A review article[12] on the structure of ABO_3 perovskite oxides concluded that such superstructure peaks are associated with the tilting BO_6 octahedra in the cubic perovskite structures. We have found similar results in several Ti-based perovskite $Ba_{1+x}Nd_{1-x}TiO_6$.[13]

The mixed valence of Eu^{2+}/Eu^{3+} was examined by Mössbauer spectroscopy. ^{151}Eu Mössbauer spectra for cubic $Eu_{1-x}Ba_xTiO_3$ ($x = 0.6,0.7$) and $Eu_{1-x}K_xTiO_3$ ($x = 0.2,0.32$) measured at room temperature were shown in Fig. 2. The experimental data for $Eu_{0.4}Ba_{0.6}TiO_3$ and $Eu_{1-x}K_xTiO_3$ ($x = 0.2,0.32$) were composed of two absorption lines, which indicated that in these samples Eu ions were present in mixed valence of Eu^{3+}/Eu^{2+}. The absorption peak with isomer shift (IS) of approximately 0 mm/s was ascribed to Eu^{3+}, while that with IS of approximately −13 mm/s was associated with Eu^{2+}. The

TABLE I. Lattice parameters for the samples obtained by high pressure and temperature.

Sample	a (nm)	c (nm)	Vo (nm^3)
$Eu_{0.2}Ba_{0.8}TiO_3$	0.398 (3)	0.400 (6)	0.0635
$Eu_{0.3}Ba_{0.7}TiO_3$	0.397 (4)		0.0629
$Eu_{0.4}Ba_{0.6}TiO_3$	0.396 (1)		0.0628
$Eu_{0.8}K_{0.2}TiO_3$	0.389 (3)		0.0590
$Eu_{0.68}K_{0.32}TiO_3$	0.389 (8)		0.0592
$La_{0.7}Na_{0.3}TiO_3$	0.388 (9)		0.0584
$La_{0.7}K_{0.3}TiO_3$	0.391 (5)		0.0598

difference of approximately 13 min/s between IS values for Eu^{3+} and Eu^{2+} could be interpreted in terms of the fact that Eu^{2+} ions have a larger shielding effect of $4f^7$ electrons on the *s* orbital in comparison with Eu^{3+} ions ($4f^6$). ^{151}Eu Mössbauer spectra shown in Fig. 2 exhibited slightly asymmetric broad single lines, and the half widths were more broadened in comparison with that of the natural single lines. These facts confirmed the presence of an unresolved quadrupole interaction. The experimental data were all well fitted by twelve transition lines,[14] and the hyperfine parameters are given in Table II. For sample $Eu_{0.3}Ba_{0.7}TiO_3$, only the absorption line with IS of approximately −13 mm/s was observed, while the absorption with IS of approximately 0 mm/s was not clear. This may be due to the presence of traces of Eu^{3+} ions in the sample. For $Eu_{04}Ba_{0.6}TiO_3$, the absorption peak associated with Eu^{3+} was slightly increased in intensity, whereas both $Eu_{0.8}K_{0.2}TiO_3$ and $Eu_{0.68}K_{0.32}TiO_3$ exhibited the strong absorption associated with Eu^{3+}. From the relative intensities of the subspectra associated with Eu^{3+} and Eu^{2+}, it can be concluded that the percentage of Eu^{3+} increased in a sequence of $Eu_{0.3}Ba_{0.7}TiO_3$, $Eu_{0.4}Ba_{0.6}TiO_3$, $Eu_{0.68}K_{0.32}TiO_3$, and $Eu_{0.8}K_{0.2}TiO_3$. Considering the starting $Eu_2{}^{3+}O_3$, it is clear that large amounts of Eu^{3+} ions were reduced during the formation of perovskite oxides doped with barium more than those doped with potassium. In other words, Eu ions at A site probably have a strong tendency to be in mixed valence in perovskite lattice with dopants of potassium ions.

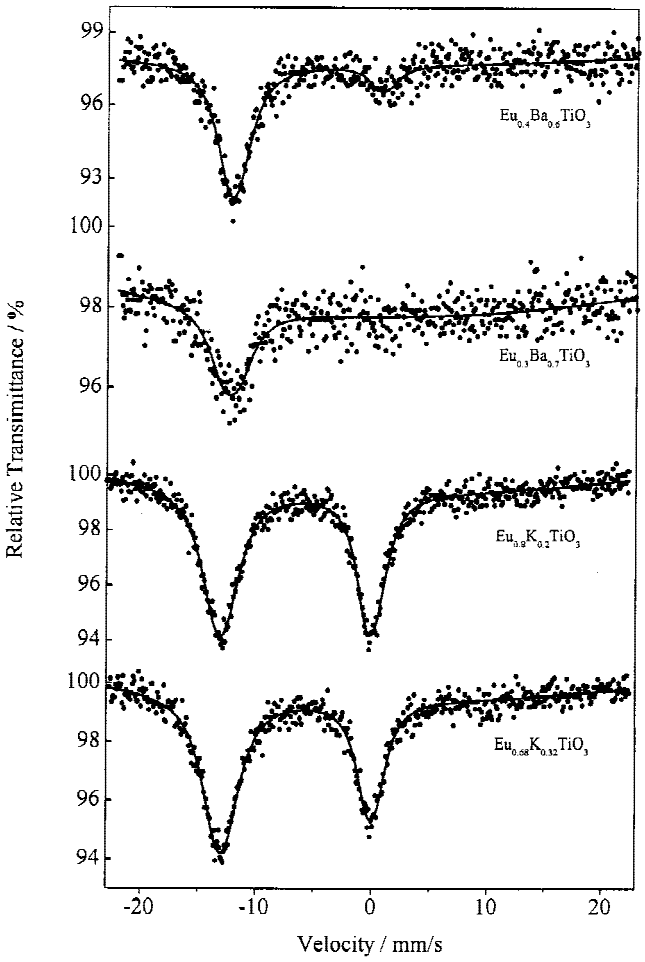

FIG. 2. ^{151}Eu Mössbauer spectra for $Eu_{1-x}Ba_xTiO_3$ (x = 0.6,0.7) and $Eu_{1-x}K_xTiO_3$ (x = 0.2,0.32). Both peaks at around −13 and 0 mm/s were associated with Eu^{2+} and Eu^{3+}, respectively.

Previous studies[15,16] have shown that Eu ions are usually in an intermediate valence state for some intermetallic compounds, in which Eu ions occupy equivalent crystallographic sites; with decreasing temperature, the corresponding ^{151}Eu Mössbauer spectra can be fitted using two single lines associated with Eu^{2+} and Eu^{3+}. At room temperature, however, both lines collapse into one single line with IS values intermediated between those of Eu^{2+} and Eu^{3+} lines. A typical example is that the IS value for Eu_3P_2 measured at room temperature is −10 mm/s; however, when temperature is decreased below 100 K, two lines with IS values equal to 0.0 and −10.6 mm/s are observed. Such a phenomenon has been named as valence fluctuation.[16] For our samples crystallizing in the perovskite structures, Eu ions probably occupied the equivalent crystallographic sites. However, two absorptions associated with Eu^{2+} and Eu^{3+} were well

TABLE II. Hyperfine parameters for the samples obtained by high pressure and temperature.

		IS (mm/s)	QS (mm/s)	FWHM (mm/s)[a]	η	I (%)
$Eu_{0.3}Ba_{0.7}TiO_3$	Eu(II)	−13.14 ± 0.08	−7.8 ± 1.3	1.38 ± 0.06	0.95 ± 0.23	100 ± 5
$Eu_{0.4}Ba_{0.6}TiO_3$	Eu(III)	−0.08 ± 0.04	−5.63 ± 0.08	1.02 ± 0.03	0.75 ± 0.16	17 ± 3
	Eu(II)	−12.99 ± 0.04	−5.5 ± 0.8	1.38 ± 0.03	0.73 ± 0.17	83 ± 2
$Eu_{0.8}K_{0.2}TiO_3$	Eu(III)	−0.06 ± 0.02	−5.7 ± 0.4	1.06 ± 0.02	0.63 ± 0.13	50 ± 3
	Eu(II)	−13.08 ± 0.02	−5.8 ± 0.3	1.52 ± 0.01	0.84 ± 0.06	50 ± 2
$Eu_{0.68}K_{0.32}TiO_3$	Eu(III)	−0.07 ± 0.03	−5.1 ± 0.4	1.04 ± 0.02	0.96 ± 0.08	45 ± 3
	Eu(II)	−13.04 ± 0.02	−5.7 ± 0.3	1.51 ± 0.01	0.84 ± 0.05	55 ± 2
Product[b]	Per.	−0.04 ± 0.04	−6.8 ± 0.5	0.93 ± 0.02	0.75 ± 0.12	44 ± 3
	Pyr.	0.56 ± 0.03	−23.5 ± 0.3	1.21 ± 0.01	0.34 ± 0.02	56 ± 2

[a]Full width half-maximum.

[b]Product was obtained by sintering the sample $Eu_{0.68}K_{0.32}TiO_3$ at 750 °C for 1 h. Per. denotes perovskite phase and Pyr. the pyrochlore phase in the decomposition product.

distinguished at room temperature, which could not be assigned to the valence fluctuation. The IS value for Eu^{2+} ions in our samples was smaller than −13 mm/s, which confirmed that the Eu^{2+}–O bonds were predominantly ionic. Similar phenomena have been found in other Eu-containing oxides, such as Eu_2VO_4 and $Eu_3V_2O_7$.[17]

The Hamiltonian representing the interaction of a nucleus with spin (I) and quadrupole moment (Q) at principal of electric-field gradient (EFG) V_{zz} is described as follows:

$$H = [eQV_{zz}/4I(2I-1)][3I_z - \mathrm{I(I+1)} + \eta(I_+^2 + I_-^2)/2] \quad , \tag{1}$$

where η is an asymmetric parameter. The fitting of the experimental data in Fig. 2 showed a negative quadrupole interaction. For the rare-earth elements, there are three contributions to V_{zz}: the first-order 4*f* contribution, the lattice contribution, and the second-order 4*f* contribution. Because Eu^{3+} ions have a ground state of $^7F_0$, the main contribution to V_{zz} should come from the latter two. For Eu^{2+}, the ground state is $^8S_{7/2}$; therefore, only the lattice contribution is appreciable. It should be mentioned that for the oxides containing Eu, the lattice contribution is usually negative. We may deduce from these facts that the lattice contribution to the EFG was larger than the second-order 4*f*. The largest absolute value of the quadrupole splitting (QS) of Eu^{2+} was 7.8 mm/s for our perovskite samples, which was smaller than that observed for Eu_2VO_4,[17] Eu_2TiO_4, and $Eu_3Ti_2O_7$.[18] This result showed that QS was strongly dependent on the crystal structure. As mentioned above, the compound $EuTiO_3$ crystallizes in the ideal cubic perovskite structure, in which the unit cell is symmetrical around axis. However, for our samples $Eu_{1-x}Ba_xTiO_3$ and $Eu_{1-x}K_xTiO_3$, the dopants (Ba or K) and host Eu ions may be distributed disorderly at A site. The positive charge centers around Eu^{3+} thus formed probably lead to the lattice distortion within a small scale due to the formation of interstitial oxygen species and cationic vacancies at A site. The symmetry around axis was thus deformed. Furthermore, nonzero η was expected. This is clearly different from that case in the parent cubic $EuTiO_3$. For Eu_2VO_4, Eu_2TiO_4, and $Eu_3Ti_2O_7$, Eu^{2+} ions are in an asymmetrical distribution around axis, showing a larger QS. For Eu^{3+} in our samples, the value of QS was near the same as that reported for other perovskite phases, such as $EuMO_3$ (M = Cr, Mn, Fe, Co, Sc),[19] $Eu_{0.2}R_{0.8}FeO_3$ (R = La, Pr, Sm, Gd, Tb, Dy, Ho, Er, Tm, Yb, Lu),[20] and $EuFe_{0.8}M_{0.2}O_3$ (M = Sc, Cr, Mn, Co).[21]

Figure 3(a) shows the room temperature EPR spectra for samples $Eu_{0.2}Ba_{0.8}TiO_3$ and $Eu_{1-x}K_xTiO_3$ (x = 0.2,0.32). Only one broad signal was observed at g = 2.00 for these samples. This signal was assigned to Eu^{2+} and cationic vacancies at A site. No signal associated with Ti^{3+} was observed at g = 1.93.[22,23] Therefore Ti ions were present as Ti^{4+} in these samples. The peak-to-peak linewidth for $Eu_{1-x}K_xTiO_3$ (x = 0.2,0.32) was much more broadened than that of $Eu_{0.2}Ba_{0.8}TiO_3$. It should be mentioned that many factors such as dipole–dipole interaction, isotropic exchange, and fine structure

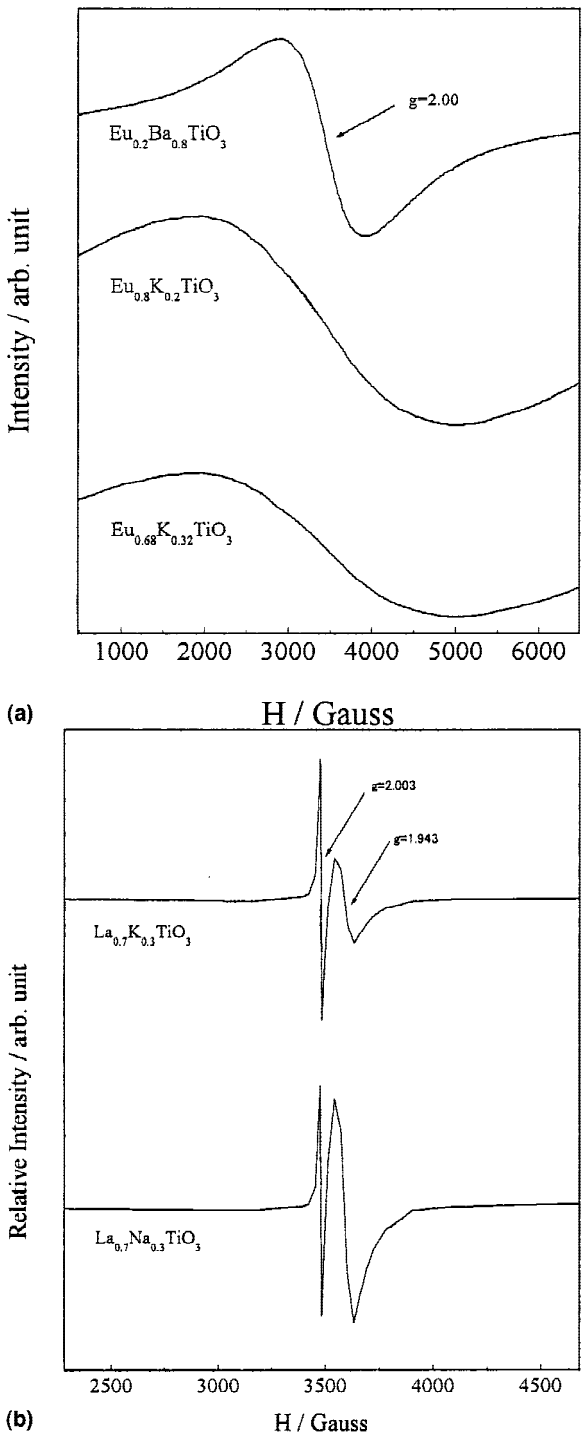

FIG. 3. EPR spectra of (a) $Eu_{0.2}Ba_{0.8}TiO_3$ and $Eu_{1-x}K_xTiO_3$ (x = 0.2,0.32) and (b) $La_{0.7}(Na,K)_{0.3}TiO_3$.

affect the linewidth of the EPR signals.[24] The dipole–dipole interactions could result in resonance line broadening, while isotropic exchange causes narrowing of the signals.[25] The linewidths for our samples were determined by the dipole–dipole interactions. For $Eu_{0.2}Ba_{0.8}TiO_3$ and $Eu_{1-x}K_xTiO_3$ ($x = 0.2,0.32$), the differences of the effective charge and ionic size of the A-site ions and the local lattice distortion would lead to the presence of an enhanced dipole–dipole interaction between Eu^{2+} ions. The larger distance between the dipolars as reflected by the slightly larger cell volume (shown in Table I) for the samples doped with Ba than that doped with K accounted for the narrowing of the resonance line in Fig. 3(a).

We also investigated the effects of the monovalence substitutions at the presence of stable trivalence rare-earth ions at A site on the valence states of Ti ions at B site under high pressure and temperature. $La_{0.7}(Na,K)_{0.3}TiO_3$ was selected as the typical samples where La^{3+} ions have a rather high valence stability at A site. From Fig. 3(b), it is clear that the EPR data for $La_{0.7}(Na,K)_{0.3}TiO_3$ exhibited two strong signals within the magnetic field of 480–6480 G. The narrower signal showed a g factor of 2.003, and the g factor for the broader signal was 1.943. On the basis of previous EPR studies on $BaTiO_3$ and doped $BaTiO_3$,[26,27] the EPR data in Fig. 3(b) can be well assigned. The signal of approximately $g = 2.00$ was due to the barium vacancies at A site, whereas the signal of approximately $g = 1.96$ was associated with Ti^{3+} ions at B site. Therefore, it can be concluded that $La_{0.7}(Na,K)_{0.3}TiO_3$ possessed cationic vacancies at A site and Ti^{3+} at B site. The vacancies at A site may be caused by loss of Na^+ and K^+ ions during the experimental procedure. Considering the starting $Ti^{4+}O_2$ and the presence of Ti^{3+} ions in $La_{0.7}(Na,K)_{0.3}TiO_3$, it is reasonable that Ti^{4+} ions were partially reduced under high pressure and temperature. This is different from that case in $Eu_{1-x}K_xTiO_3$, in which Ti^{4+} ions have a relatively high stability.

From the above, it is clear that Ti^{4+} ions exhibited different stabilities during the synthesis of Ti-based perovskite oxides by high pressure and temperature. For $La_{1-x}(Na,K)_xTiO_3$, charge compensation resulted by the substitution of lower valence ions (K^+ or Na^+) can be achieved by the valence from reduction Ti^{4+} to Ti^{3+} ions and cationic vacancies at A site. That is to say, Ti ions at B site in $La_{1-x}(Na,K)_xTiO_3$ could be present in mixed valence of Ti^{3+}/Ti^{4+}. However, Eu^{3+} ions at A site might be readily reduced by the synthesis of $Eu_{1-x}Ba_xTiO_3$ ($x = 0.6$–0.8) and $Eu_{1-x}K_xTiO_3$ ($x = 0.2,0.32$), in which the valence state of Ti ions remained constant as Ti^{4+} at B site. The different valence stabilities were probably related to the ionic sizes and charges of the dopants in the perovskite framework, but also to the atomic configuration of Eu and Ti ions. This is because the standard reduction potential for Eu^{3+} to Eu^{2+} is -0.36 eV, whereas that for Ti^{4+} to Ti^{3+} is -0.055 eV in solution according to the reaction $TiOH^{3+} + H^+ + e \Leftrightarrow Ti^{3+} + H_2O$.[28] In another words, Ti^{3+} ions can be readily obtained in solution, while Eu^{2+} can be stabilized by reduction of Eu^{3+} during high pressure and temperature.

B. Structural stabilities and thermal behaviors of $Eu_{1-x}K_xTiO_3$

Figure 4 shows the TG curve for a typical cubic sample $Eu_{0.68}K_{0.32}TiO_3$ measured in air. A weight gain of approximately 1.4% was observed in a temperature interval of 550–740 °C. To investigate the influence of heat treatment on the structure of $Eu_{0.68}K_{0.32}TiO_3$, the XRD pattern for the product obtained by sintering $Eu_{0.68}K_{0.32}TiO_3$ at 750 °C for 1 h was measured. As shown in Fig. 5, the sintered product was a mixture of perovskite and pyrochlore phases. According to the assignments of the XRD data in Fig. 5, the decomposition process could be described in the following path.

$$Eu_{0.68}K_{0.32}TiO_3 \rightarrow 0.64\ Eu_{0.5}K_{0.5}TiO_3 + 0.18\ Eu_2Ti_2O_7 \quad . \qquad (2)$$

From this path, the theoretical weight gain is approximately 1.36%, in good agreement with our experimental result (approximately 1.4%). Therefore, the decomposition for $Eu_{0.68}K_{0.32}TiO_3$ was accompanied by an oxidation process from Eu^{2+} to Eu^{3+}.

^{151}Eu Mössbauer spectrum for the decomposition product of $Eu_{0.68}K_{0.32}TiO_3$ is shown in Fig. 6. The experimental data exhibited a very broad asymmetry line, which was associated with Eu^{3+}. Fitting the experimental data showed that Eu^{3+} ions occupied at two lattice sites. Their isomer shift values were -0.04 and 0.56 mm/s, and quadrupole splitting values were -6.8 and

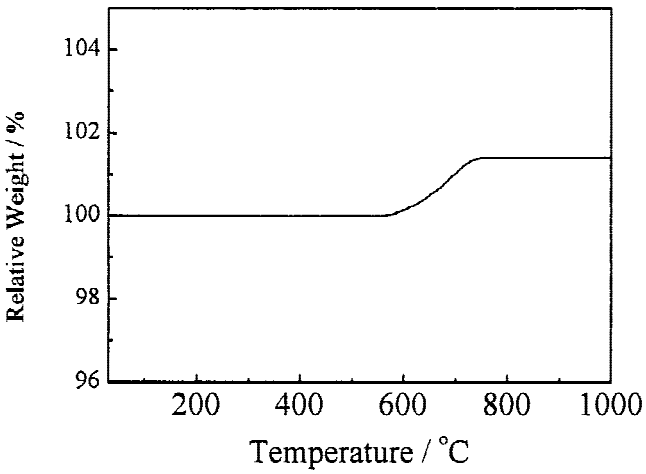

FIG. 4. TG curve for sample $Eu_{0.68}K_{0.32}TiO_3$ measured in air.

−23.5 mm/s, respectively. It is well known that both RE sites and Ti sites in cubic pyrochlores $RE_2Ti_2O_7$ (where RE is a rare earth) have the threefold rotational symmetry. The EFGs at RE sites in $RE_2Ti_2O_7$ are the largest in all rare-earth-containing compounds.[29] A quadrupole splitting of −21.33 mm/s is reported for $Eu_2Ti_2O_7$ in Ref. 30. Therefore, the component with the large absolute value of quadrupole splitting could be assigned to Eu^{3+} in $Eu_2Ti_2O_7$ and the other one to Eu^{3+} in $Eu_{0.5}K_{0.5}TiO_3$. Similar to the above discussion on $Eu_{0.8}K_{0.2}TiO_3$ and $Eu_{0.68}K_{0.32}TiO_3$, the nonzero quadrupole splitting for $Eu_{0.5}K_{0.5}TiO_3$ was closely related to the random distribution of Eu and K ions at A site in the cubic perovskite lattice. If the difference of recoil factors of Eu ions in perovskite and pyrochlore oxides was neglected, the numbers of Eu ions in both oxides should be in direct proportion to the area ratio of two components. From Table II, it can be seen that the percentage of Eu ions in the perovskite and pyrochlore phase reached 44 and 56%, respectively, which was in good agreement with the theoretical value of 47 and 53% from our proposed decomposition process in Eq. (2).

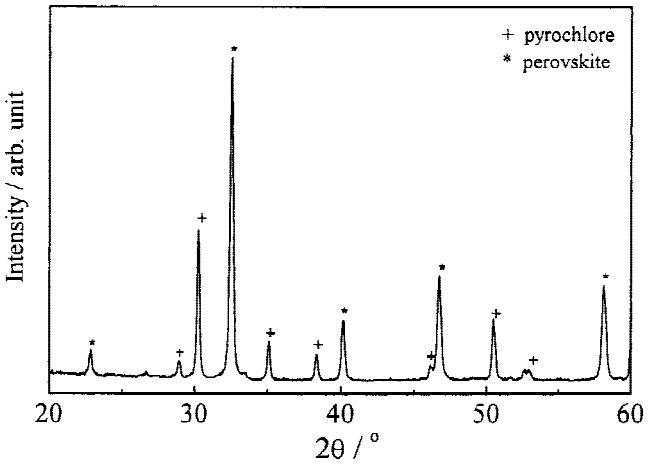

FIG. 5. XRD pattern for the decomposition product of $Eu_{0.68}K_{0.32}TiO_3$ at 750 °C for 1 h. Asterisks and crosses denote the perovskite and pyrochlore phases, respectively.

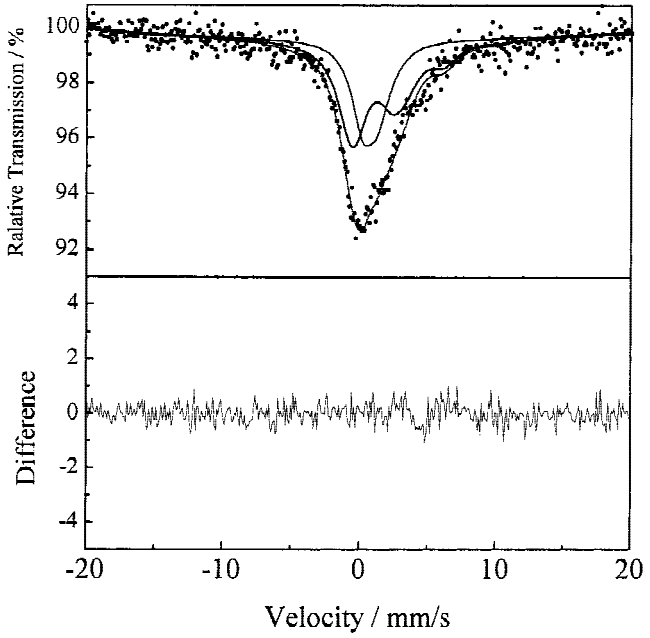

FIG. 6. ^{151}Eu Mössbauer spectrum for the decomposition product of $Eu_{0.68}K_{0.32}TiO_3$ at 750 °C for 1 h.

IV. CONCLUSIONS

The mixed valence characteristics and structural stabilities of the typical titanium perovskite oxides obtained by high pressure and temperature were studied. The following conclusions were obtained from the present study.

(i) With increasing Ba content, $Eu_{1-x}Ba_xTiO_3$ underwent a phase transformation from cubic ($x = 0.6,0.7$) to tetragonal ($x = 0.8$).

(ii) Eu ions at A site in titanium-based perovskite lattice exhibited a mixed valence of Eu^{2+}/Eu^{3+}, whereas Ti ions were present in pure Ti^{4+} at B site.

(iii) When A site ions contained stable La^{3+}, Ti ions at B site showed a mixed valence of Ti^{3+}/Ti^{4+}.

(iv) Cubic $Eu_{0.68}K_{0.32}TiO_3$ was metastable. At 750 °C, it decomposed into a mixture of perovskite and pyrochlore phases accompanied by an oxidation process from Eu^{2+} to Eu^{3+}.

ACKNOWLEDGMENT

This project was financially supported by funding from NSFC (No. 19804005) (L.L.).

REFERENCES

1. A. Jayaraman, in *Handbook on the Physics and Chemistry of Rare Earth*, edited by K.A. Gschneidner Jr. and L. Eyring (North-Holland Amsterdam, 1978), p. 707.
2. J. Zhou, Chinese J. High Pressure Phys. **6,** 7 (1992).
3. G. Gemazeau, and B. Buffat, Mater. Res. Bull. **16,** 1465 (1981).
4. H. Choy, G. Demazeau, J.M. Dance, S.H. Byeon, and K.A. Muller, J. Solid State Chem. **109,** 289 (1994).
5. L. Li, Q. Wei, H. Liu, D. Zheng, and W. Su, Z. Phys. B **96,** 451 (1995).
6. L. Li, G. Li, Y. Che, and W. Su, Chem. Mater. **12,** 2567 (2000).
7. S. Feng, G. Li, L. Li, and X. Li, Rev. High Pressure Sci. Technol. **7,** 1362 (1998).
8. C.C. Hays, J.S. Zhou, J.T. Markert, and J.B. Goodenough, Phys. Rev. B **60,** 10367 (1999).
9. J.E. Sunstrom and S.M. Kauzlarich, Chem. Mater. **5,** 1539 (1993).
10. H. Yamamoto, T. Tahara, Y. Sugagara, K. Kuroda, and C. Kato, Phase Transitions **41,** 137 (1993).
11. W.F. McLune, editor, Powder Diffraction File: Inorganic Phases: JCPDS International Center for Powder Diffraction Data, Swarthmore, PA, Card No. 9-127, 34-596, 1989.

12. M.T. Anderson, K.B. Greenwood, G.A. Tailor, and K.R. Poeppelmeimer, Progr. Solid State Chem. **122,** 197 (1993).
13. L. Li, G. Li, X. Song, and W. Su, Chin. Phys. Lett. **15,** 925 (1998).
14. W. Su, X. Liu, M. Jin, W. Xu, D. Wu, and M. Liu, Phys. Rev. B **37,** 35 (1988).
15. M. Croft, J.A. Hodges, E. Kemmly, A. Krishnan, V. Murgai, and L.C. Gupta, Phys. Rev. Lett. **48,** 826 (1982).
16. H. Raffius, B.D. Mosel, W.W. Muller, U. Pegelow, J.W. Hadenfeldt, and T. Vomhof, J. Phys. Chem. Solids **55,** 219 (1994).
17. Z.M. Stadnik, G. Stroink, and T. Arakawa, Phys. Rev. B **44,** 12552 (1988).
18. C.L. Chien, S. DeBenedetli, and F. De S. Barros, Phys. Rev. B **10,** 3913 (1974).
19. T.C. Gibb, J. Chem. Soc. Dalton. Trans. 2245 (1981).
20. M. Jin, X. Liu, W. Zhang, and W. Su, Solid State Commun. **76,** 985 (1990).
21. X. Liu, M. Jin, and M. Liu, Hyperfine Interact. **68,** 237 (1991).
22. W.L. Warren, C.H. Seager, D. Dimos, and E.J. Friebele, Appl. Phys. Lett. **61,** 253 (1992).
23. I.P. Bykev, M.D. Glinchuk, V.V. Skorokhod, and V.M. Kurland, Ferroelectrics **127,** 89 (1992); J. Huang, N.D. Chasteen, and J.J. Fitzgerald, Chem. Mater. **10,** 2848 (1998).
24. L. Li, G. Li, R.L. Smith Jr., and H. Inomata, Chem. Mater. **12,** 3705 (2000).
25. J.H. Van Fleck, Phys. Rev. **74,** 1168 (1948).
26. T.R.N. Kutty, P. Murugaraj, and N.S. Gajbhiye, Mater. Res. Bull. **20,** 565 (1985).
27. T.R.N. Kutty, P. Murugaraj, and N.S. Gajbhiye, Mater. Lett. **2,** 396 (1984).
28. R.L. David, editor, *CRC Handbook of Chemistry and Physics*, 74th ed. (CRC Press, Boca Raton, FL), Table 8–21.
29. E.R. Bauminger, A. Diamant, I. Felver, I. Nowik, and S. Ofer, Phys. Lett. **A50,** 321 (1974).
30. C.L. Chien and A.W. Sleight, Phys. Rev. B **18,** 2031 (1978).